文章编号: 1001 - 9014(2015)06 - 0641 - 06

DOI:10.11972/j.issn.1001 - 9014.2015.06.001

Electrical crosstalk in InGaAs focal plane array

LI Dong-Xue[1], WANG Tian-Meng[1], SHEN Wen-Zhong[1], ZHANG Yue-Heng[1*], LI Xue[2], LI Tao[2]

(1. Key Laboratory of Artificial Structures and Quantum Control (Ministry of Education), Department of Physics and Astronomy, Shanghai Jiao Tong University, Shanghai 200240, China;
2. State Key Laboratories of Transducer Technology, Shanghai Institute of Technical Physics, Chinese Academy of Sciences, Shanghai 200083, China)

Abstract: Crosstalk characteristic is closely correlated to higher sensitivity and higher resolution imaging of focal plane array (FPA). The electrical crosstalk of typical planar and mesa $In_{0.53}Ga_{0.47}As$/InP FPAs as a function of illumination wavelength, incidence, as well as the etching depth in the mesa structures was investigated quantitatively in detail by simulation. It was demonstrated that mesa structures possess better electrical crosstalk characteristics compared with the planar designs. Significantly, the crosstalk is lower for shorter wavelength radiation while the front-side illumination devices show better electrical crosstalk characteristics than do the back-side illuminated devices. It is ascribed to the influence of material absorption depth and the p-i junction depletion width of such structures. It was also found that the electrical crosstalk appears to be greatly suppressed when the etching depth of the mesa structure covers the entire absorption layer of the device. The results suggest design rules for InGaAs FPA with low electrical crosstalk.

Key words: $In_{0.53}Ga_{0.47}As$/InP focal plane array, electrical crosstalk, planar structure, mesa structure

PACS: 42.79.Pw

InGaAs 焦平面探测器电串音性能的研究

李冬雪[1], 王天盟[1], 沈文忠[1], 张月蘅[1*], 李 雪[2], 李 淘[2]

(1. 上海交通大学 物理与天文系 人工结构及量子调控教育部重点实验室, 上海 200240;
2. 中国科学院上海技术物理研究所 传感技术国家重点实验室, 上海 200083)

摘要: 串音与焦平面阵列(FPA)的灵敏度和分辨率密切相关. 用模拟的方法定量地计算了 $In_{0.53}Ga_{0.47}As$/InP 探测器焦平面阵列的电串音随光波波长、入射方向和台面的刻蚀深度的变化情况. 结果显示台面结构的器件的串音抑制性能比平面结构的要好. 明显地发现短波长的光串音较小, 正照射的串音比背照射要小, 这是由材料吸收深度和异质结耗尽层宽度的影响造成的. 另外, 当台面的刻蚀深度穿透吸收层厚度时, 其电串扰几乎完全被抑制. 研究结果提出了相应的 InGaAs FPA 的低串音设计.

关 键 词: $In_{0.53}Ga_{0.47}As$/InP 焦平面阵列; 电串音; 平面结构; 台面结构

中图分类号: TN215 **文献标识码**: A

Introduction

Photodiode arrays are critically important to short-wave infrared (SWIR) light sensing applications in telecommunication, defense, and industrial systems. Photodiode arrays made of lattice matched $In_{0.53}Ga_{0.47}As$/InP materials, used for SWIR imaging, are particularly attractive because they are relatively economical, respond rapidly to light amplitude modulation, and are extremely sensitive at common eye-safe illumination laser wavelengths[1-2]. In recent years, the format and demand for

Received date: 2014 - 09 - 28, **revised date**: 2015 - 09 - 24 **收稿日期**:2014 - 09 - 28, **修回日期**:2015 - 09 - 24

Foundation items: Supported by 863 Program of China (2011AA010205), National Major Basic Research Project (2011CB925603), Natural Science Foundation of China (91221201, 61234005, 11074167)

Biography: LI Dong-Xue (1991-), female. Heze, China, master degree. Research fields focus on imaging performance of semiconductor infrared detector. E-mail: dongxue8660002@163.com

* **Corresponding author**: E-mail: yuehzhang@sjtu.edu.cn

such detector arrays have increased dramatically while the pixel density increases and the pitch of these devices has been dramatically reduced[3].

Crosstalk between the individual elements of an infrared sensing array occurs when the absorbed photons in a particular detector of the array generates a signal in another detector element. Under the influence of crosstalk, the array's image resolution and light sensitivity become worse as the pitch of the detector array is reduced[4]. The question of how to mitigate crosstalk is significant in modern $In_{0.53}Ga_{0.47}As$/InP FPA′s imaging technologies. However, to date, few investigations have been reported on InGaAs FPA crosstalk analysis[4-5].

Crosstalk is often differentiated by its electrical and optical traits. Optical crosstalk is the result of photon refraction, reflection, external and internal scattering in the illuminated detector elements toward undesired neighboring detector elements. Electrical crosstalk results from carriers that are photons generated under one detector diffuse towards the other detector element where they are collected. The electrical crosstalk is influenced by device structure parameters such as array pitch and device geometry. Moreover, it is usually the electrical crosstalk, which can be influenced by modifying the array's structural traits, that we can address readily with appropriate device design[6].

In this paper, we study the electrical crosstalk of $In_{0.53}Ga_{0.47}As$/InP FPA with planar and mesa structures by numerical simulation.

1 Simulation

There are two kinds of structures that are frequently adopted in InGaAs FPAs: the planar and the mesa structures. The schematic diagrams of these structures are shown in Fig. 1.

The planar structure detector is mainly made up of n-InP/i-$In_{0.53}Ga_{0.47}As$/n-InP (cap/absorption/buffer) epitaxial materials. Then, the p-diffusion region is formed through the n-InP cap layer to produce a p-i-n junction. The n-InP cap layer in this design is 0.5 μm thick with the doping concentration target of 5×10^{16} cm^{-3}.

The mesa structure detector is made up of p-InP/i-$In_{0.53}Ga_{0.47}As$/n-InP (cap/absorption/buffer) epitaxial materials that are cap and absorption layer etched. The etching depth is the InGaAs absorption layer etching depth excluding the prior etching of the cap p-layer as shown in Fig. 1(b). The p-InP cap layer in this design is 0.5 μm thick with the doping concentration target of 1×10^{19} cm^{-3}.

In order to simplify the simulations, only three InGaAs photodiode pixels are simulated which are labeled as anodes 1, 2, and 3. The width of the p-diffusion windows is 15 μm. The buffer layers are 1 μm thick n-InP with a donor concentration target of 2×10^{18} cm^{-3}. The absorption layers are all 2.5 μm thick, lattice matched i-$In_{0.53}Ga_{0.47}As$ to InP with a target background donor concentration of 1×10^{15} cm^{-3}.

To further simplify the simulations, we consider only the electrical crosstalk when light is incident on the center pixel. Therefore, for our purposes, we define

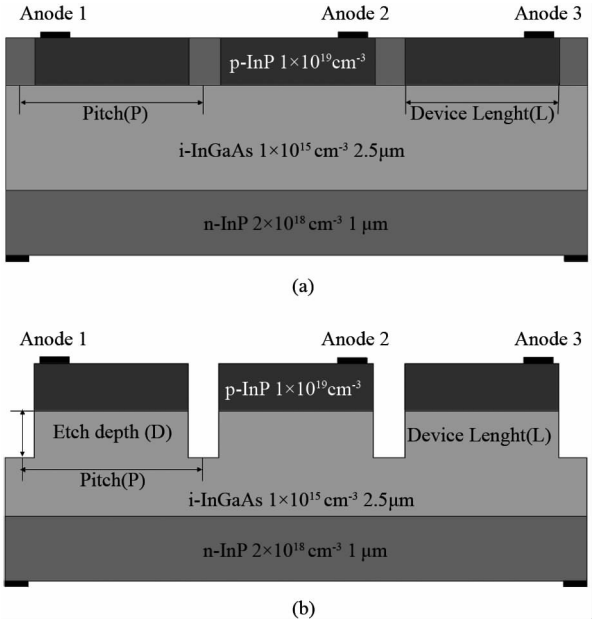

Fig. 1 Schematic diagrams of (a) planar structure, and (b) mesa structure $In_{0.53}Ga_{0.47}As$/InP FPA.

图 1 (a) $In_{0.53}Ga_{0.47}As$/InP FPA 的平面结构示意图, (b) $In_{0.53}Ga_{0.47}As$/InP FPA 的台面结构示意图

crosstalk as:

$$\text{Crosstalk} = 10\log\left(\frac{I_{\text{Anode1}} + I_{\text{Anode3}}}{I_{\text{Anode2}}}\right), \quad (1)$$

where I_{Anode1}, I_{Anode2}, and I_{Anode3} are the net photocurrents measured at Anode1, Anode2, and Anode3, respectively.

The current density can be written as the sum of electrons and holes current densities:

$$\vec{J}_{\text{Total}} = \vec{J}_{\text{n}} + \vec{J}_{\text{p}}. \quad (2)$$

Three kinds of recombination mechanisms, *i. e.* optical radiative, shockley-read-hall(SRH) and surface recombination are used in the simulation.

Table 1 Physical parameters used in the simulation

表 1 计算中使用的部分物理参数

Parameters	$In_{0.53}Ga_{0.47}As$	InP
Radiative recombination coefficient	9.6×10^{-11} cm^3/s	1.2×10^{-10} cm^3/s
Minority carriers lifetime	10 μs	0.2 ns
Mobility of electrons/holes	10 000/200 $cm^2/(V\cdot s)$	As a function of doping[7]
Saturation velocities of electrons/holes	$2\times10^7/7.7\times10^6$ cm/s	$2.5\times10^7/1\times10^6$ cm/s

Some physical parameters used in the simulation are shown in Table 1. In the following simulations, the electrical crosstalk characteristics of $In_{0.53}Ga_{0.47}As$/InP FPA are obtained at the reverse bias of 0.3 V. The incident light is monochromatic with a spot size of 5 μm and uniform intensity of 70 pW.

2 Results and discussion

In order to verify the reliability of the simulation,

the internal quantum efficiency and response of $In_{0.53}Ga_{0.47}As$/InP PIN photodiode were calculated at first, as shown in Fig. 2. The IQE was calculated by:

$$IQE = \frac{I_{Anode}}{I_{Available\ Photocurrent}}, \quad (3)$$

where I_{Anode} is the generated photocurrent in anode, $I_{Available\ Photocurrent}$ is a measure of the photo absorption in the device expressed as a current. It is shown that the calculated $In_{0.53}Ga_{0.47}As$/InP photodiodes are responsive between 0.9 and 1.68 μm at room temperature. The simulated results agree well with the experimental results of Sensors Unlimited, Inc., Goodrich ISR Systems[8], indicating that the results of photocurrent and selection of parameters are reasonable and correct. This ensures that the resulting calculation of crosstalk is also reliable.

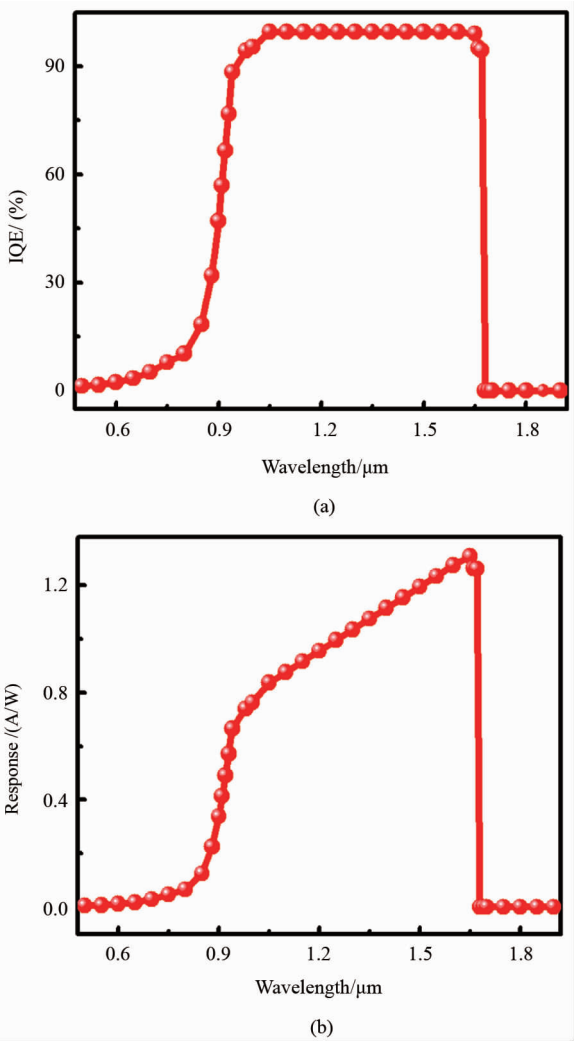

Fig. 2　(a) The internal quantum efficiency (IQE) as a function of wavelength, (b) The spectral response of simulated $In_{0.53}Ga_{0.47}As$/InP PIN photodiode

图 2　(a) $In_{0.53}Ga_{0.47}As$/InP PIN 光电二极管的内量子效率(IQE)随波长的变化，(b) $In_{0.53}Ga_{0.47}As$/InP PIN 光电二极管的光谱响应

Light at 1.3 μm (O band) and 1.5 μm (C band) are important eye-safe infrared wavelengths for telecommunications, medicine, and laser ranging that achieve near optimal sensitivity when using InGaAs detector technologies. Therefore, we calculate the electrical crosstalk at 1.3 μm and 1.5 μm for the outlined planar and mesa structures.

Figure 3 shows the electrical crosstalk of the simulated devices as a function of pixel pitch. The mesa structure in these simulations has an InGaAs etching depth of 0.8 μm. It is clear that the exponential trend of electrical crosstalk changes with pixel pitch independently of device structure and wavelength. In addition, the crosstalk of the planar array simulations is higher than that of the mesa array simulations for the same pitch independently of illumination wavelength. This is because mesa array with appropriate etching depth could suppress the generated carrier lateral diffusion effectively. Taking 1.5 μm as an example, when the pitch is 20 μm, the electrical crosstalk of mesa structure InGaAs FPA is about 5dB lower than that of the planar structure. These crosstalk results suggest that if pixel size of the planar FPA is 15 μm and distance between pixels is 5 μm, only about 0.3% (0.1% for mesa structure) of the signal current on the center pixel will be laterally diffused into the neighbor pixels. Therefore, in order to reduce the electrical crosstalk of InGaAs FPAs, mesa structures are a better choice when potential passivation difficulties are ignored.

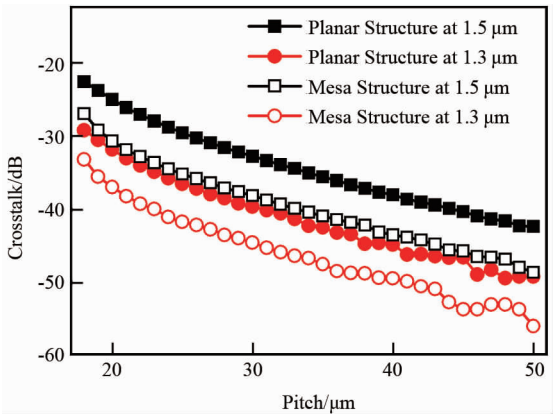

Fig. 3　The electrical crosstalk of planar and mesa structure InGaAs FPA at 1.5 μm and 1.3 μm wavelength for front-side illumination.

图 3　1.5 μm 和 1.3 μm 的光正面照在平面和台面结构时的电串音比较

Similar conclusions that electrical crosstalk in mesa structure HgCdTe(MCT) FPA is lower than that of planar FPA were shown previously[6]. Compared with HgCdTe(MCT) FPAs, the lower electrical crosstalk of an InGaAs FPA is often favorable. Typically, a MCT FPA has a higher electrical crosstalk than an InGaAs FPA because of its increased diffusion current associated with the intrinsically lower resistance-area product (R_0A) of MCTs[9].

It should be noted that for a given structure, the crosstalk at 1.5 μm is always higher than that at 1.3 μm illumination, suggesting the FPA electrical crosstalk of

these devices also varies with illumination wavelength. Our simulations show that the electrical crosstalk of planar and mesa structures at 1.3 μm illumination is about 7dB lower than that at 1.5 μm illumination. The photon number of 1.5 μm illumination is only 1.15 times larger than that of 1.3 μm illumination. Therefore, the resultant difference of crosstalk, which is approximately 5 times larger, suggests photon number is not the reason for the crosstalk difference between these wavelengths. However, the absorption depths within the InGaAs layer at 1.5 μm and 1.3 μm illuminations are 1.49 μm and 0.54 μm, respectively, while the depletion width in the p-i junction is about 1.3 μm at the voltage bias of -0.3V. Thus for 1.3 μm light, carriers are generated mostly in the p-i junction depletion region and do not laterally diffuse because of the built-in electric field. This results in lower electrical crosstalk at lower wavelength illuminations.

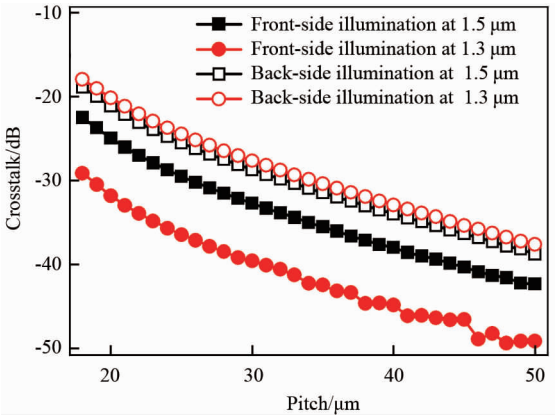

Fig. 4 The electrical crosstalk of planar InGaAs FPA illuminated from front-side and back-side orientation at 1.5 μm and 1.3 μm wavelength.
图4 InGaAs FPA在正照射与背照射的电串音比较

To verify the above theory of the depletion width and the absorption depth, we further compared the electrical crosstalk of planar structures illuminated at 1.5 μm and 1.3 μm from front-side and back-side orientations. Front-side illumination represents light incident through the p-InP cap layer, while back-side illumination represents light incident through the n-InP buffer layer. The results of those simulations are presented in Fig. 4. When illuminated from the front-side, the electrical crosstalk of 1.5 μm light is about 7dB (5 times) higher than that at 1.3 μm light. However, when illuminated from back-side, almost all of carriers are generated outside of the p-i junction for 1.3 μm light. In contrast, part of the carriers are generated in the p-i junction for 1.5 μm, leading to slight difference of about 1dB (1.3 times) between the two wavelengths.

For 1.5 μm illumination, there is about 4 dB (2.5 times) difference between front-side and back-side crosstalk. In contrast, the difference is 11dB (12 times) for 1.3 μm light. The results indicate that back-side illumination has a worse electrical crosstalk compared with the case of the front-side illumination for all the absorbed light wavelength. In addition, this crosstalk difference is more pronounced for wavelengths with shorter absorption depth.

Note that we did not consider the influence of the n-i junction because that its effect can be ignored when compared with that of the p-i junction. This is demonstrated by the simulated built-in drift field of the planar structure with and without bias as shown in Fig. 5. In the junction between the high doping $1\times10^{19}\,cm^{-3}$ p-InP cap layer and i-InGaAs absorption layer, the built-in electric potential is 1.05 V, whereas it is 0.35 V between the n-i junction when the bias is 0 V. When the device is reverse biased to 0.3 V, the drift field is still concentrated on the p-i junction side as shown in Fig. 5(b). In addition, the depletion width of the n-i junction is only about 0.2 μm, which is small compared with that of the p-i junction and is much smaller than the absorption depth at both 1.3 μm and 1.5 μm illumination wavelengths. These observations suggest that most of the light absorption happens outside of the n-i junction, which can therefore be largely ignored in our analysis of these devices.

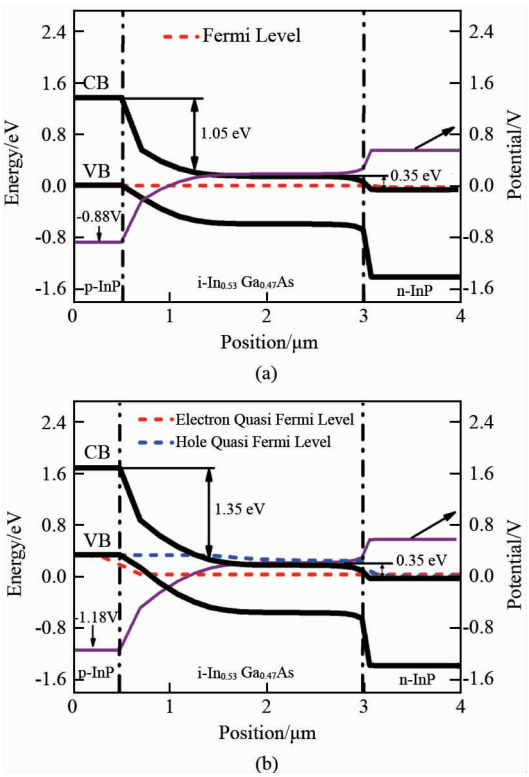

Fig. 5 The band diagram of $In_{0.53}Ga_{0.47}As$/InP PIN (a) without bias, and (b) with reverse bias of 0.3 V. The corresponding potentials of $In_{0.53}Ga_{0.47}As$/InP PIN are also shown.
图5 (a) $In_{0.53}Ga_{0.47}As$/InP PIN在零电压时的能带图,(b) $In_{0.53}Ga_{0.47}As$/InP PIN在-0.3 V电压时的能带图

Modern commercial InGaAs FPA manufacturers typically adopt back-side illumination FPAs that are flip chip interconnection bonded to readout integrated circuits (ROIC). In such devices, increasing the p-i junction depletion depth by using higher purity InGaAs is an alternative way to reduce the electrical crosstalk of the tradi-

tional back-side illumination modes.

In Fig. 6, the electrical crosstalk simulation results of mesa structure InGaAs FPA structures are shown. We studied the effect of different etching depths when the illumination wavelength is 1.5 μm, the device length is 15 μm, and the pixel pitch is 20 μm. As expected, the electrical crosstalk of the mesa structure InGaAs FPA is suppressed by increasing the etching depth through the InGaAs layer.

There are several mechanisms we proposed to explain this result. First, with increasing InGaAs etching depth, the interface recombination at the etched walls increases. This means the recombination rate of photon generated carriers increases and thus the effective minority carrier concentration is reduced. Second, with increasing etching depth, the effective absorption volume of InGaAs becomes smaller, so that the number of photon generated carriers is reduced. The above two factors decrease of the concentration of photon generated carriers, and in turn result in a decrease of electrical crosstalk for mesa structure InGaAs FPAs. A third candidate mechanism is that as etching depth increases, pixels become more isolated and photon generated carriers have less opportunity to diffuse laterally. Thus the electrical crosstalk of mesa structure InGaAs FPAs is suppressed by increasing its etching depth. Similarly, deep trench isolation (DTI) structures in mature complementary metal oxide silicon (CMOS) imaging devices demonstrates that its electrical crosstalk is suppressed by increasing trench depth[10].

As shown in Fig. 6(b), when the etching depth is equal to the InGaAs absorption layer thickness, the electrical crosstalk of mesa structure InGaAs FPA is close to nil. At this time, the optical crosstalk will be the major component of the crosstalk. We should note that, the deepest etching depth maybe not the best mesa structure considering the optical crosstalk. The optimal etching depth should be balanced between the electrical crosstalk and the optical crosstalk.

3 Conclusions

The electrical crosstalk of typical planar and mesa $In_{0.53}Ga_{0.47}As$/InP FPAs as a function of illumination wavelength, incidence, as well as the etching depth in the mesa structures was investigated quantitatively in detail by simulation. The calculated internal quantum efficiency and responsivity traits are consistent with practical InGaAs devices. The simulations show the crosstalk at eye-safety illumination wavelengths of 1.5 μm is higher than that at 1.3 μm for both planar and mesa structures due to the absorption depth differences between these wavelengths. Compared with front-side illumination, back-side illumination shows higher electrical crosstalk, and exerts a greater influence for the monochromatic light that has a shorter absorption depth. It was also found that the electrical crosstalk characteristics of mesa structures are better than that of planar ones at any wavelength, provided that they demonstrate similar traits. And it can be suppressed by increasing the etching depth through the InGaAs layer. These results present a guidance for low crosstalk design of InGaAs FPA.

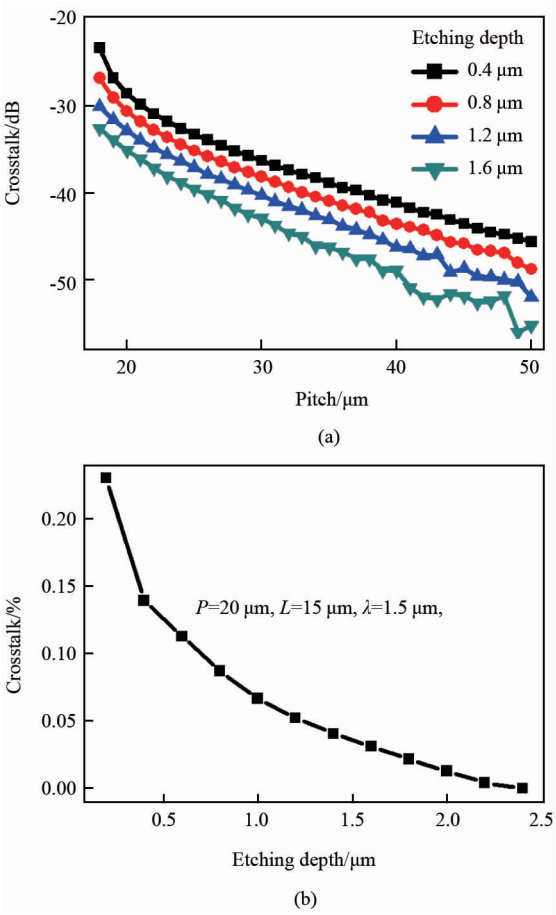

Fig. 6　(a) The dependence of electrical crosstalk on pixel pitch at different etching depths for front-side illuminated mesa structure InGaAs FPA, (b) The dependence of electrical crosstalk on etching depth for front-side illuminated mesa structure InGaAs FPA

图 6　(a) 不同吸收层刻蚀深度的 InGaAs FPA 台面结构的电串音随像元间距的变化, (b) InGaAs FPA 台面结构的电串音随吸收层刻蚀深度的变化

Acknowledgements

We acknowledge the contribution of Professor H. C. Liu, who was the former teacher and mentor of the authors and passed away in October 2013. This paper is dedicated to his memory. In addition, we would like to thank Dr. Sean Hinds for his fruitful discussions and suggestions. This work was supported in part by the 863 Program of China (2011AA010205), the National Major Basic Research Projects (2011CB925603), and the Natural Science Foundation of China (91221201, 61234005, and 11074167).

References

[1] HUANG Song-Lei, ZHANG Wei, HUANG Zhang-Cheng, *et al*. The noise of extended wavelength InGaAs FPA with large perimeter-area-ratio [J]. *Journal of Infrared and Millimeter Waves* (黄松垒, 张伟, 黄张成, 等. 大周长面积比延伸波红 InGaAs 红外焦平面噪声, **外与毫米波学报**), 2012, **31**(3): 235-238.

[2] ZHU Yao-Ming, LI Yong-Fu, LI Xue, *et al*. Extended-wavelength 640x1 linear InGaAs detector arrays using N-on-P configuration for

back illumination [J]. *Journal of Infrared and Millimeter Waves*(朱耀明,李永富,李雪,等. 基于 N-on-P 结构的背照射延伸波长 640 × 1 线列 InGaAs 探测器, 红外与毫米波学报)2012, **31**(1):11 - 1431.

[3] CTON D, JACK D M, SESSLER T. Large format short-wave infrared (SWIR) focal plane array (FPA) with extremely low noise and high dynamic range[J]. *Proc. of SPIE*, 2009, **7298**:72983E - 72983E - 72913.

[4] ZHU Yao-Ming, LI Xue, WEI Jun *et al.* Analysis of cross talk in high density mesa linear InGaAs detector arrays using tiny light dot[J]. *Proc. of SPIE*, 2012, **8419**:84191I.

[5] Application note of Goodrich, Crosstalk limits in monolithic InGaAs photodiode arrays, *Rev. B*, 2006, 1 - 4.

[6] Musca C A, Dell J M, Faraone L, *et al.* Analysis of crosstalk in HgCdTe p-on-n heterojunction photovoltaic infrared sensing arrays[J]. *Journal of Electronic Materials*, 1999: **28**.

[7] Sotoodeh M, Khalid A H, Rezazadeh A A. Empirical low-field mobility model for III-V compounds applicable in device simulation codes [J]. *Journal of Applied Physics*, 2000, **87**:2890.

[8] Dixon P, Masaun N, Evans M, *et al.* Monolithic planar InGaAs detector arrays for uncooled high-sensitivity SWIR imaging[J]. *Proc. of SPIE*, 2009, **7307**:730706 - 730706 - 730712.

[9] Cohen M J, Olsen G H. Room temperature InGaAs camera for NIR imaging[J], *Infrared Detectors and Instrumentation*, 1993, **1946**: 436 - 443.

[10] Park B J, Jung J, Moon C.-R, *et al.* Deep trench isolation for crosstalk suppression in active pixel sensors with 1.7 μm pixel pitch [J], *Japanese Journal of Applied Physics*, 2007, **46**: 2454 - 2457.